CONCEPTUAL DESIGN OF REACTIVE DISTILLATION COLUMNS USING STAGE COMPOSITION LINES

Matthias Groemping, Ramona-M Dragomir* and Megan Jobson***

** Degussa AG, Hanau, Germany
* Department of Process Integration, UMIST, Manchester, UK

A conceptual design methodology for the synthesis of reactive distillation columns is presented. The method assesses feasibility of a proposed reactive distillation column, designs the column and allows evaluation of the design for both fully reactive and 'hybrid' column configurations. Stage composition lines are used to represent all possible liquid compositions in a column section, for specified product compositions and for all reflux or reboil ratios. Reaction equilibrium is assumed on each reactive stage, and vapour-liquid equilibrium is assumed on all stages. The graphical column design method allows fast and relatively simple screening of different reactive distillation column configurations. The methodology is illustrated by application to an ideal reactive system and for MTBE production.

KEYWORDS: transformed composition space, feasibility, hybrid column

INTRODUCTION

Distillation with chemical reaction has received attention as an alternative to conventional processes; reactive distillation has proved to be an economical alternative in many applications (*e.g.* MTBE and TAME synthesis, production of methyl acetate, manufacture of di-isopropyl ether, oligomerisation of linear butenes and removal of butadiene through dimerisation).

Process synthesis for reactive distillation includes design and optimisation of the column. Because of the interactions between reaction and distillation in the combined unit, the modelling and design of reactive distillation is complex. The reaction influences the composition on each tray, and thus mass transfer and vapour and liquid loads; for homogeneously catalysed reactions, the liquid hold-up is another important design parameter, because the reaction extent is not only a function of tray compositions and temperature, but also of residence time. An alternative approach, which is adopted in this work, is to assume that the reaction equilibrium is achieved on each stage.

The aims of process synthesis for reactive distillation columns are to identify promising column designs for a given feed mixture and a given set of desired products. Conceptual methods, such as that developed in this paper, frequently use graphical representation of important design variables, which allows the design engineer to gain insights into the process and to guide the development of promising process designs.

ESTABLISHED CONCEPTUAL DESIGN TOOLS FOR REACTIVE DISTILLATION

Reaction Space and Transformed Compositions

For systems with equilibrium reactions, any feasible composition in a reactive section of a column will always lie on the reactive equilibrium surface (or *reaction space* [1]). This space represents the subset of mole fraction space for which both phase and reaction equilibrium conditions are satisfied. To map reaction space to mole fraction space requires calculation of reactive bubble points for the combined chemical and phase equilibrium condition. It is assumed that the reaction takes place only in the liquid phase.

Each reaction reduces the number of degrees of freedom (DOF) according to the Gibbs phase rule for isobaric systems [*e.g.* 2]:

$$\mathrm{DOF} = 1 + C - \pi - R \qquad (1)$$

Mixtures with two degrees of freedom, even those with more than three components, will have a two-dimensional reaction space; this space can be mapped onto a two-dimensional plane in *transformed composition space* [3-5]. For each reaction, one component, the reference component, can be eliminated from the concentration space. The benefit of using transformed compositions is that graphical methods can be applied to mixtures with more than three components, as long as the reaction space is at most two-dimensional. In this work we will use the definition for transformed composition proposed by Ung and Doherty [4]:

$$X_i = \frac{x_i - \nu_i^T \cdot \nu_{ref}^{-1} \cdot x_{ref}}{1 - \nu_{tot}^T \cdot \nu_{ref}^{-1} \cdot x_{ref}} \qquad \forall\ i = 1,\ldots,C-R-1, \qquad (2)$$

The equilibrium surface of an etherification reaction A+B$\leftrightarrow$C with inert component D in shown in mole fraction space (Fig. 1(a)) and in transformed composition space (Fig. 1(b)). Components A and B are selected as independent components and are used as co-ordinates of the reaction space. Component C is the reference component. The transformed composition of component D can be calculated from [4]:

$$\sum_{\substack{i \neq \text{reference} \\ \text{component C}}} X_i = 1 \qquad (3)$$

Two edges of Fig. 1(b) represent the non-reactive binary pairs AD and BD. The third edge represents the equilibrium line of the ternary system A, B, C.

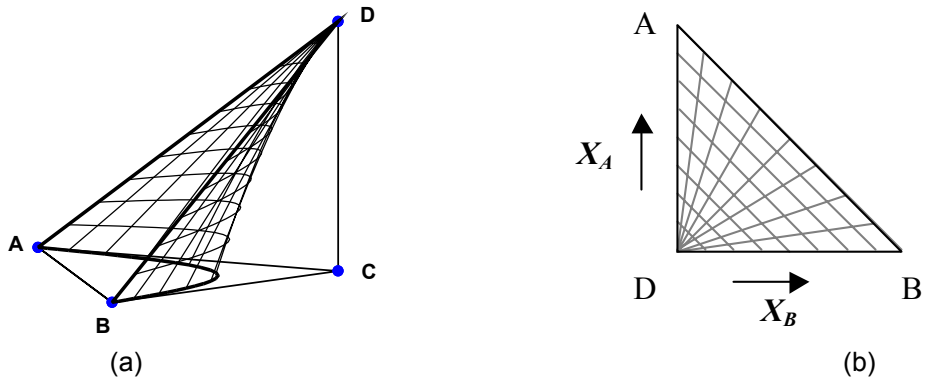

Fig. 1 Equilibrium surface for an etherification reaction A+B↔C with inert component D (a) mole fraction space; (b) transformed composition space (reference component C).

Fig. 2(a) displays the equilibrium surface of an esterification reaction A+B↔C+D in mole fraction space. Because all components can exist in their pure form, the reaction space contains all components, even though it is a two-dimensional surface. The reaction space can therefore be represented as a square, as shown in Fig. 2(b). Components A and B are selected as independent components and are used as co-ordinates of the reaction space; component C is the reference component; component D is calculated from eq. (3). The transformed compositions representing pure D, are $X_A = 0$; $X_B = 0$; $X_D = 1$, so that pure D is located at the lower left-hand corner of the square. The transformed compositions representing pure C are $X_A = 1$; $X_B = 1$; $X_D = -1$; so that pure C is located at the upper right-hand corner. The edges of the square represent the non-reactive binary pairs AC, AD, BC, BD. While transformed compositions can be negative, their sum is always unity.

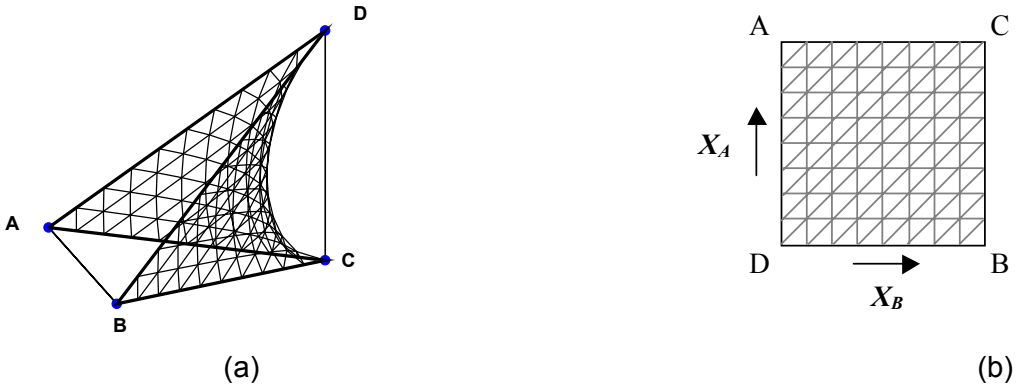

Fig. 2 Equilibrium surface for an esterification reaction A+B↔C+D (a) mole fraction space; (b) transformed composition space (reference component C).

Graphical Design Methods for Reactive Distillation

Graphical methods have been developed to assess the feasibility of a proposed column, for both reactive and non-reactive distillation columns, for a given pair of products. These methods require a continuous composition profile to link the two product compositions in composition space. That is, points on the composition profiles of the rectifying section and the stripping section must coincide if the proposed separation is feasible (*e.g.* Fig. 3). An alternative formulation, proposed for non-reactive systems [6], uses the *stage composition line*, which is the locus of liquid

compositions on a given stage number in a column section, for any reflux or reboil ratio, to obtain a product of specified composition. Stage composition lines are continuous loci, unlike composition profiles, which are sets of discrete points. Therefore, intersection of continuous profiles is easier to obtain than finding points on two profiles that coincide.

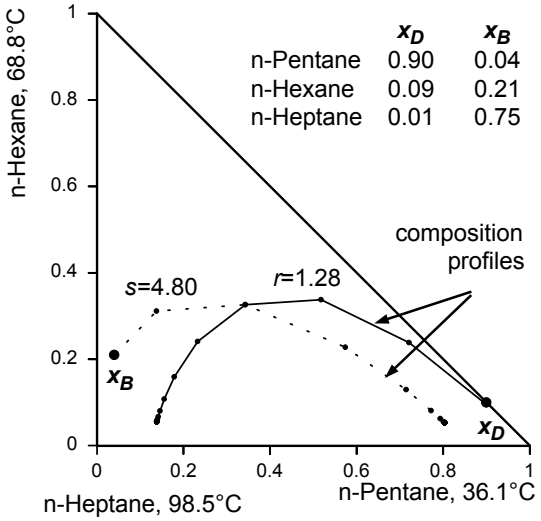

Fig. 3 Non-reactive feasibility test: Points on composition profiles of the rectifying and stripping sections must coincide [6].

The set of all feasible composition profiles in a column section corresponding to a specified product is bounded by the total reflux curve and the pinch point curve. These two curves correspond to extreme modes of column operation: total reflux and thermodynamically optimum operation [5, 7]. The pinch point curve, for both reactive and non-reactive systems can be determined, given the vapour-liquid equilibrium and reaction space of the system. The region of feasible composition profiles, for non-reactive mixtures, was named the *operation leaf* of the column section [8] (as shown, for example, in Fig. 4).

Analogies between non-reactive ternary distillation and two-dimensional reactive distillation have been profitably exploited [*e.g.* 9]. Based on these analogies, design methods using composition profiles for single and double feed columns [3, 10] have been developed, including for the case that inert (non-reactive) components are present [11]. Design methods for hybrid columns, *i.e.* those containing both reactive and non-reactive sections [12] have also been developed. A limitation of existing approaches is that it is difficult to obtain points on composition profiles which coincide exactly; instead, intersection of the profiles (between discrete stage compositions) is often taken as the criterion for feasibility. Kinetically controlled reactive distillation columns have also been addressed [13-16], but these methods are restricted to single reactions.

No comprehensive approach to systematically generate and evaluate column designs has been developed for reactive distillation with two degrees of freedom, equilibrium reactions and for fully reactive and hybrid columns, or for two-phase feeds. This work presents a new methodology that overcomes some of the limitations and trial-and-error of previous approaches for reactive distillation columns

(both fully reactive and hybrid columns) with two degrees of freedom and equilibrium reactions. The approach allows the feed to be introduced to a single stage or between two stages. Multiple designs, which can easily be evaluated, are generated.

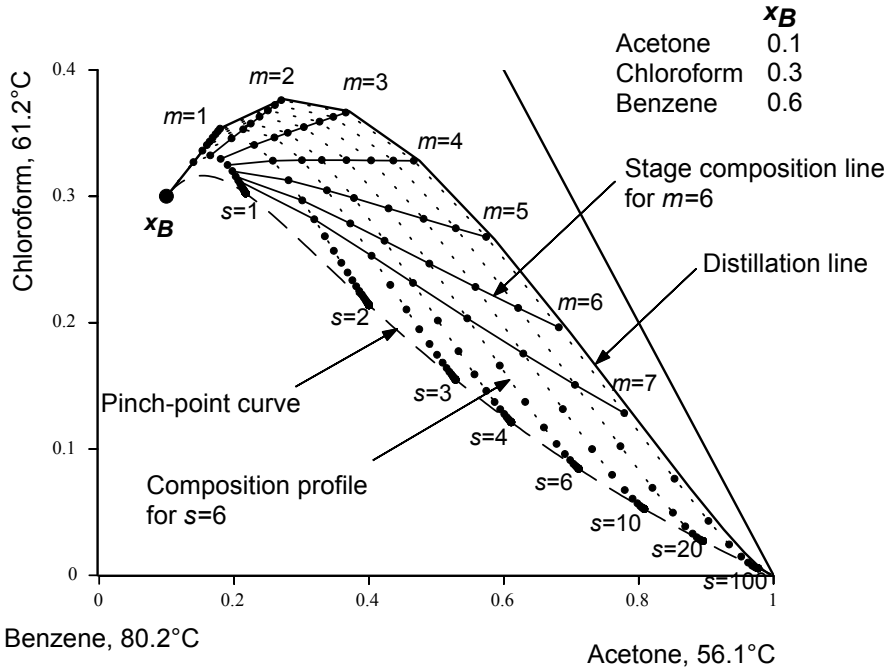

Fig. 4 Stage composition lines, composition profiles and operation leaf for a non-reactive stripping section [8].

REACTIVE DISTILLATION DESIGN USING STAGE COMPOSITION LINES

This work defines reactive stage composition lines and develops a conceptual design methodology for systems with two degrees of freedom according to the Gibbs phase rule for isobaric systems (eq. 1), *i.e.* ternary non-reactive systems or reactive systems with three independent components. The methodology is applicable to non-hybrid and hybrid reactive distillation columns, featuring multiple equilibrium reactions, with a single feed and two products. The method can be applied for feasibility analysis, column design and to quickly evaluate design options. Constant molar overflow is assumed, but the method can easily be extended to overcome this limitation.

Reactive Stage Composition Lines and Reactive Operation Leaves

In this work we define by analogy the *reactive stage composition line* as the locus of compositions leaving a certain reactive stage at any reboil or reflux ratio. Reactive stage composition lines are continuous lines, as the reflux or reboil ratio can be varied continuously. This is an advantage of stage composition lines over composition profiles, as all points on a stage composition line are attainable and satisfy the specified product composition.

Stage composition lines and composition profiles have the same bounds. By analogy to the operation leaf for non-reactive systems, we define the region of all liquid compositions achievable in a reactive column section for a given product

composition the *reactive operation leaf*. In well-behaved cases, the reactive operation leaf is bounded by the reactive total reflux curve and the reactive pinch point curve [5].

Fig. 5 illustrates the chemical equilibrium surface and reactive distillation line map are shown in mole fraction space for an ideal mixture of four components (a, b, c and d). Component c decomposes into a and b (c $\leftrightarrow$ a + b) and d is an inert component. The products of the reaction are the most and least volatile components. The number of degrees of freedom for this system is two, as there are four components, two phases and one reaction.

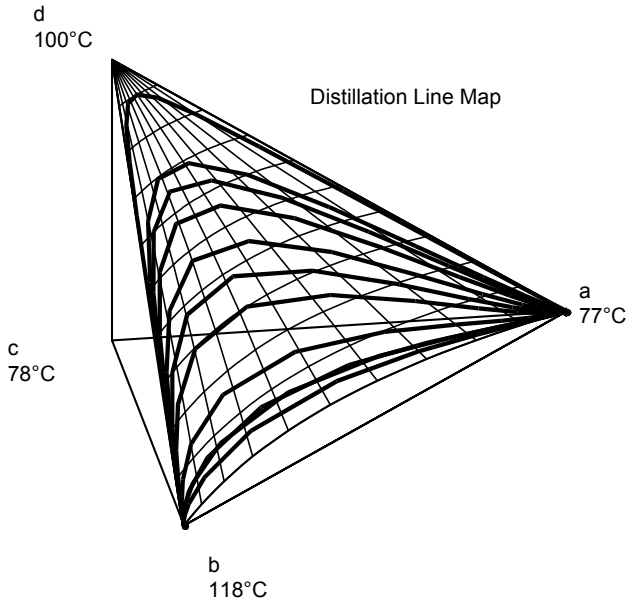

Fig. 5 Chemical equilibrium surface (grid of thinner lines) and reactive distillation line map (thicker lines lying on surface). Decomposition reaction c $\leftrightarrow$ a + b with inert component d.

Fig. 6 shows the reactive operation leaf, composition profiles and stage composition lines in transformed composition space for the bottom product specified in Table 1. Reactant c is the reference component. For large reboil ratios the reactive composition profiles approximate the reactive distillation line, and for a large number of stages the reactive stage composition lines approximate the reactive pinch point curve.

Table 1 Feed and product data for ideal decomposition reaction example.

Com-ponent	Stoichio-metry	Non-reactive boiling point	Distillate		Bottoms		Feed (above stage)	
	ν [-]	T_B [°C]	X_D transf.	x_D mole fr.	X_B transf.	x_B mole fr.	X_F transf.	x_F mole fr.
a	-1	77	0.950 (#)	0.9489	0.005 (#)	0.0026	0.488	3.2E-6
c	1	78	-	0.0224	-	0.0024	-	0.9520 (#)
d	0	100	0.005 (#)	0.0051	0.045 (#)	0.0451	0.025	0.0480
b	-1	118	0.045 (#)	0.0236	0.950 (#)	0.9499	0.488	0.0 (#)

(#)specified values

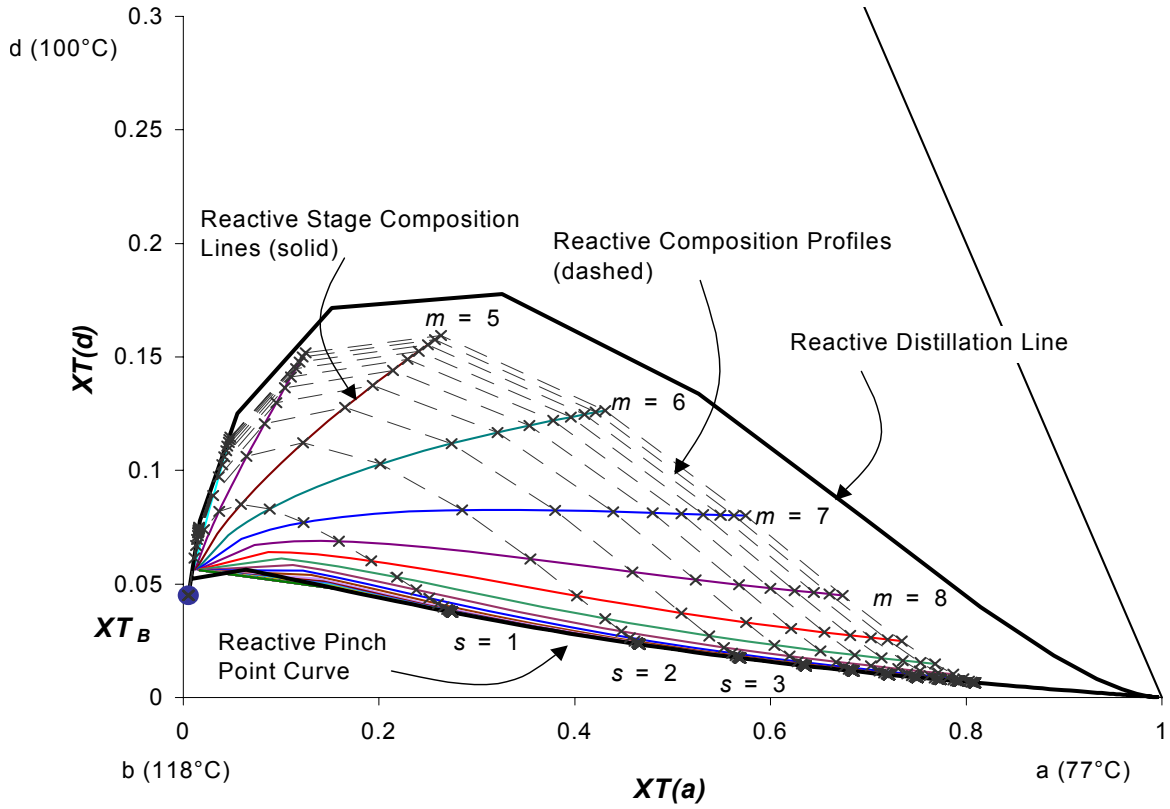

Fig. 6 Reactive operation leaf, reactive stage composition lines and reactive composition profiles for the bottom product given in Table 1.

Stage composition lines are often approximately straight as long as the reactive pinch point curve and the reactive distillation line do not intersect; this observation has not been explained. In many cases, therefore, stage composition lines can be approximated using relatively few values for the reflux or reboil ratio, between which the stage composition line can be interpolated. Only a few points are required to plot the approximate reactive stage composition lines, even if the reboil ratio is varied from zero to infinity.

In cases where the reactive pinch point curve and the reactive distillation line intersect, the resulting stage composition lines are not linear and a greater number of segments should be used to approximate the stage composition lines. Fig. 7 shows such a case. In these special cases, composition profiles may lie within the concave region between the reactive pinch point curve and the reactive distillation line, as well as within the area bounded by the reactive distillation line and the reactive pinch point curve.

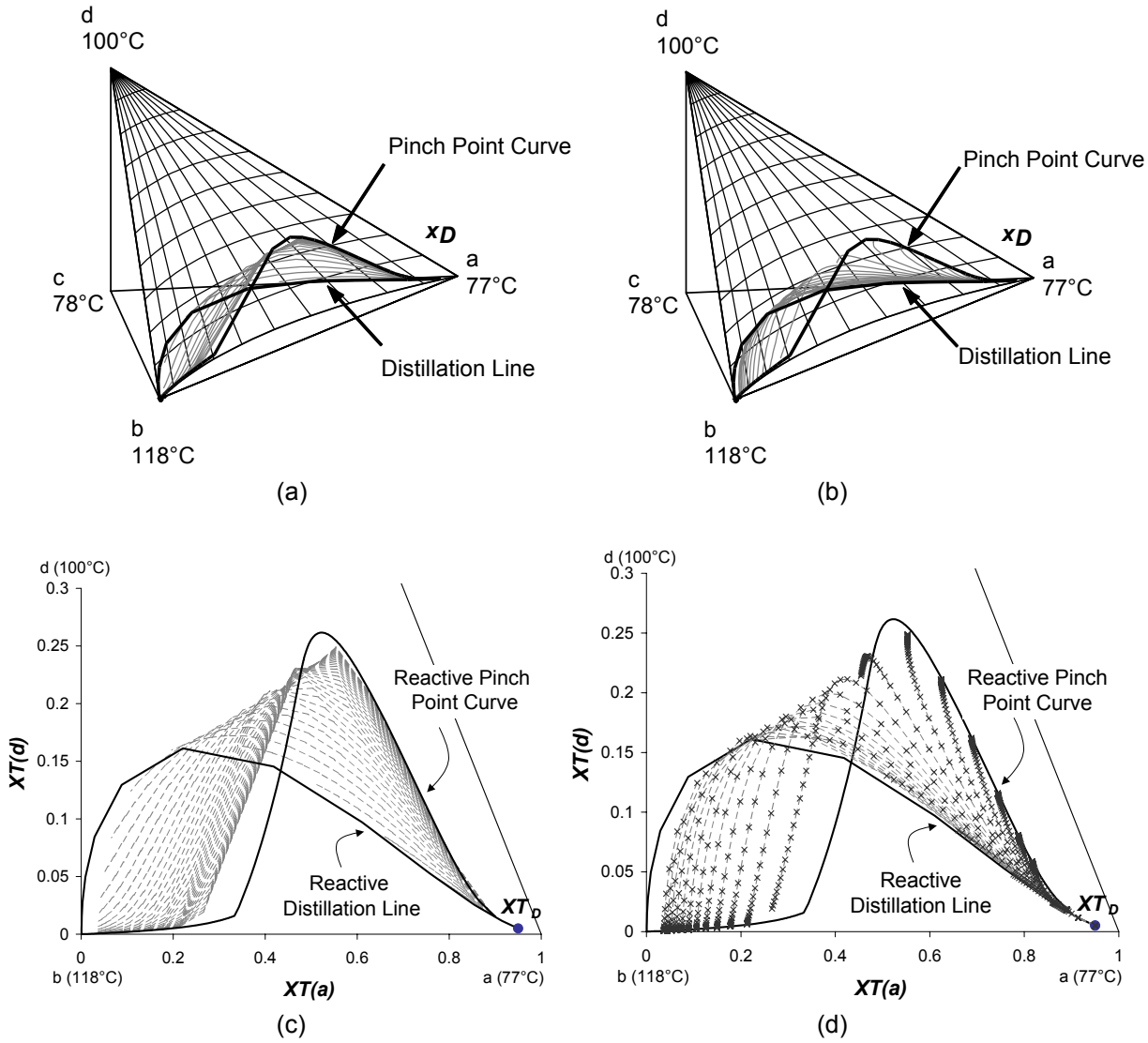

Fig. 7 Reactive operation leaf for the top product x_D. (a) stage composition lines, mole fraction space; (b) composition profiles, mole fraction space; (c) stage composition lines, transformed space; (d) composition profiles, transformed space. (System as in Fig. 5)

Fig. 8 shows both the stripping and the rectifying operation leaves for this example. That the two operation leaves overlap indicates feasibility of the split [5, 7]. The feasibility test using operation leaves is not conclusive, because compositions lying outside the bounds of the pinch point curve and distillation line can also be achieved.

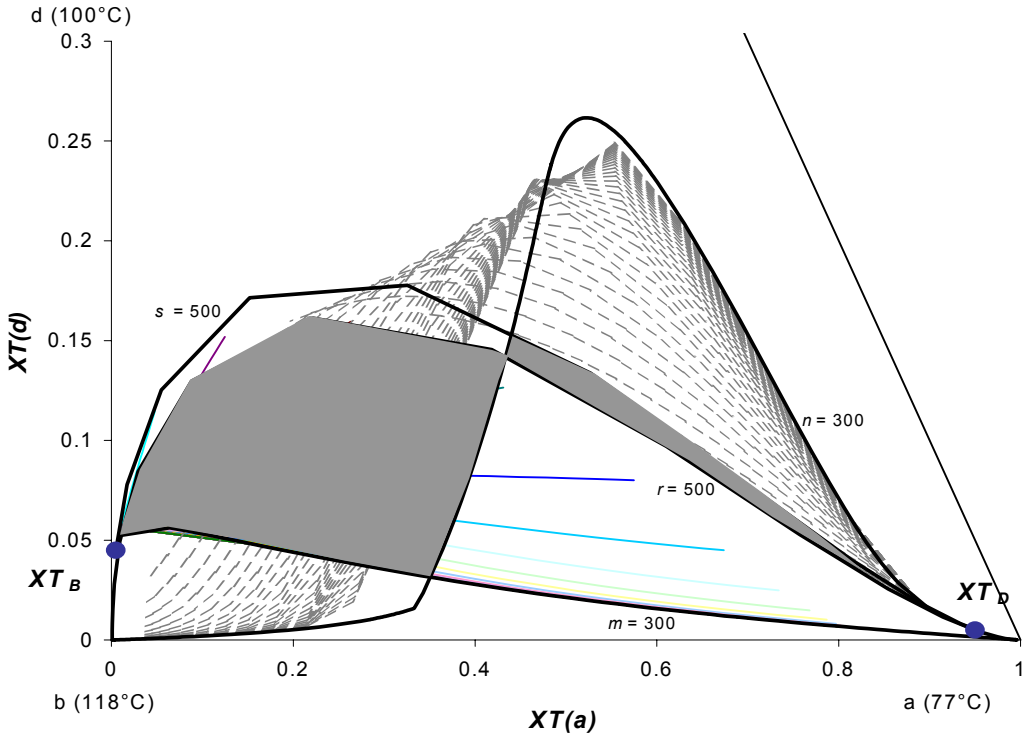

Fig. 8 Overlap of rectifying and stripping operation leaves (shaded area) indicates feasibility of the split. System as in Figs 5 to 7.

Calculation of Reactive Stage Composition Lines

Stage composition lines use the information contained in a series of composition profiles at different values of the reflux or reboil ratio. Fig. 9 shows the rectifying and stripping sections and the definition of streams entering and leaving each section.

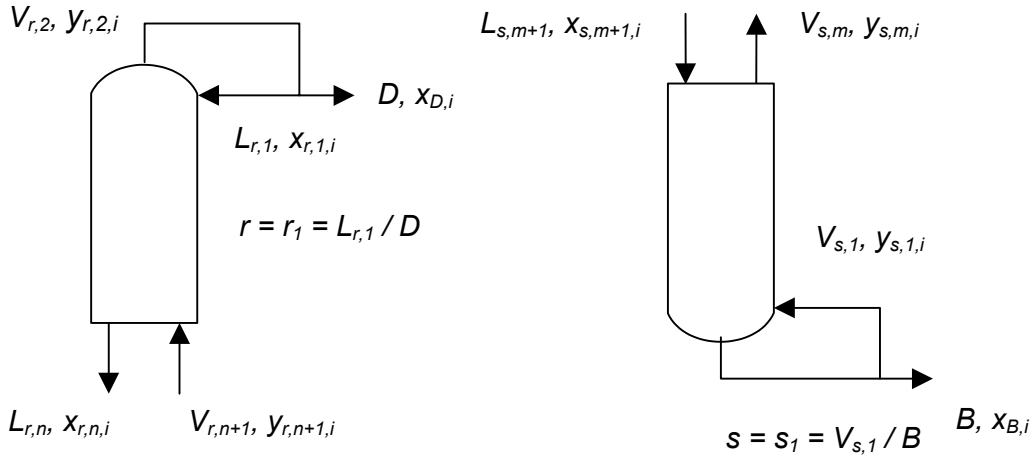

Fig. 9 Rectifying and stripping sections for generating composition profiles

A short derivation of the equations governing the reactive composition profiles is given below. The operating line for the reactive rectifying section in terms of transformed compositions (based on Barbosa and Doherty [3]) is given by:

$$Y_{r,n+1,i} = \frac{\frac{R_n}{\kappa_{rx}}}{1+\frac{R_n}{\kappa_{rx}}} \cdot X_{r,n,i} + \frac{1}{1+\frac{R_n}{\kappa_{rx}}} \cdot X_{D,i} \qquad \forall\, i = 1,\ldots,C-R-1 \qquad (4)$$

and that of the reactive stripping section by:

$$X_{s,m+1,i} = \frac{\left(\frac{S_m+1}{\kappa_{sx}}-1\right)}{1+\left(\frac{S_m+1}{\kappa_{sx}}-1\right)} \cdot Y_{s,m,i} + \frac{1}{1+\left(\frac{S_m+1}{\kappa_{sx}}-1\right)} \cdot X_{B,i} \qquad \forall\, i = 1,\ldots,C-R-1 \qquad (5)$$

where κ are dimensionless parameters relating the reference component concentrations above or below stages *n* or *m*, respectively, to the reference component product compositions:

$$\kappa_{rx} = \frac{1-\nu_{tot}^{T} \cdot \nu_{ref}^{-1} \cdot x_{D,ref}}{1-\nu_{tot}^{T} \cdot \nu_{ref}^{-1} \cdot x_{r,n,ref}} \qquad (6)$$

$$\kappa_{sy} = \frac{1-\nu_{tot}^{T} \cdot \nu_{ref}^{-1} \cdot y_{s,m,ref}}{1-\nu_{tot}^{T} \cdot \nu_{ref}^{-1} \cdot x_{B,ref}} \qquad (7)$$

$$\kappa_{sx} = \frac{1-\nu_{tot}^{T} \cdot \nu_{ref}^{-1} \cdot x_{B,ref}}{1-\nu_{tot}^{T} \cdot \nu_{ref}^{-1} \cdot x_{s,m+1,ref}} \qquad (8)$$

$$\kappa_{ry} = \frac{1-\nu_{tot}^{T} \cdot \nu_{ref}^{-1} \cdot y_{r,n+1,ref}}{1-\nu_{tot}^{T} \cdot \nu_{ref}^{-1} \cdot y_{r,2,ref}} \qquad (9)$$

$$\kappa_{rD} = \frac{1-\nu_{tot}^{T} \cdot \nu_{ref}^{-1} \cdot x_{r,1,ref}}{1-\nu_{tot}^{T} \cdot \nu_{ref}^{-1} \cdot x_{D,ref}} \qquad (10)$$

$$\kappa_{rD2} = \frac{1-\nu_{tot}^{T} \cdot \nu_{ref}^{-1} \cdot x_{D,ref}}{1-\nu_{tot}^{T} \cdot \nu_{ref}^{-1} \cdot y_{r,2,ref}} \qquad (11)$$

The definitions for the transformed reflux ratio R_n and the transformed reboil ratio S_m on stage *n* and *m,* respectively, differ from those of Barbosa and Doherty [3], and are:

$$R_n = \left[\left(r_1 \cdot \kappa_{rD} + 1\right) \cdot \kappa_{ry} - 1\right] \cdot \kappa_{rx} \qquad (12)$$

$$S_m = \left(s_1 \cdot \kappa_{sy} + 1\right) \cdot \kappa_{sx} - 1 \qquad (13)$$

The molar liquid and vapour flow rates in a reactive rectifying or stripping section are simple functions of the transformed reflux and reboil ratios:

$$\frac{L_{r,n}}{D} = R_n \tag{14}$$

$$\frac{L_{s,m+1}}{B} = S_m + 1 \tag{15}$$

Assuming constant molar overflow and liquid phase reactions, the vapour flow rate in the rectifying section depends only on the external reflux ratio r_1 and the change of flow rate due to reaction in the condenser, expressed by κ_{rD} and κ_{rD2}, where κ_{rD} and κ_{rD2} are unity for a total condenser. The molar vapour flow rates in the column sections can be calculated from:

$$\frac{V_{r,n+1}}{D} = \frac{V_{r,2}}{D} = \left(r_1 \cdot \kappa_{rD} + 1\right) \cdot \kappa_{rD2} \tag{16}$$

$$\frac{V_{s,m}}{B} = \frac{V_{s,1}}{B} = s_1 \tag{17}$$

Alternate application of the operating line and reactive bubble point or dew point calculations generates section profiles. After calculating a series of profiles at different values of the reflux or reboil ratio and collating the results, the stage composition lines can be obtained.

Criteria for Feasibility of Proposed Products

Julka and Doherty [17] derived a feasibility criterion for a proposed separation, assuming that the feed is introduced to a single tray: the composition of the liquid (or vapour) entering the stripping stage has to be exactly the same as that leaving the rectifying section. This feasibility criterion is valid for both non-reactive distillation columns and reactive distillation columns featuring equilibrium reactions, irrespective of the feed quality, the number of components, the influence of heat effects, the number of liquid phases or the number of chemical equilibrium reactions. Fig. 10(a) illlustrates the basis for this feasibility criterion.

For two-phase feeds, it is most practical to inject the feed between two stages [18], as shown in Fig. 10(b). The criterion of Julka and Doherty [17] is only approximate in this case. We develop an additional feasibility criterion, which is valid for feeds introduced between two stages.

For a feasible design, the overall balances have to be satisfied. There are *C*–*R* independent material balances over the column:

$$\overline{F} = \overline{D} + \overline{B} \tag{18}$$

$$X_{F,i} = \frac{\overline{D}}{\overline{F}} \cdot X_{D,i} + \left(1 - \frac{\overline{D}}{\overline{F}}\right) \cdot X_{B,i} \qquad \forall\, i = 1,\ldots,C-R-1 \tag{19}$$

The transformed flow rates (indicated by a bar, *e.g.* $\overline{F}$) are related to the real molar

flows (*e.g. F*) [3]. There is one degree of freedom between the variables *D/F, B/F,* $x_{F,i\neq ref}$. The overall balances (eqs. 18 and 19) calculate the feed concentrations and product flow rates, given the product compositions, feed concentrations of the reference components and one other specification (*i.e. D/F, B/F* or $x_{F,i\neq ref}$).

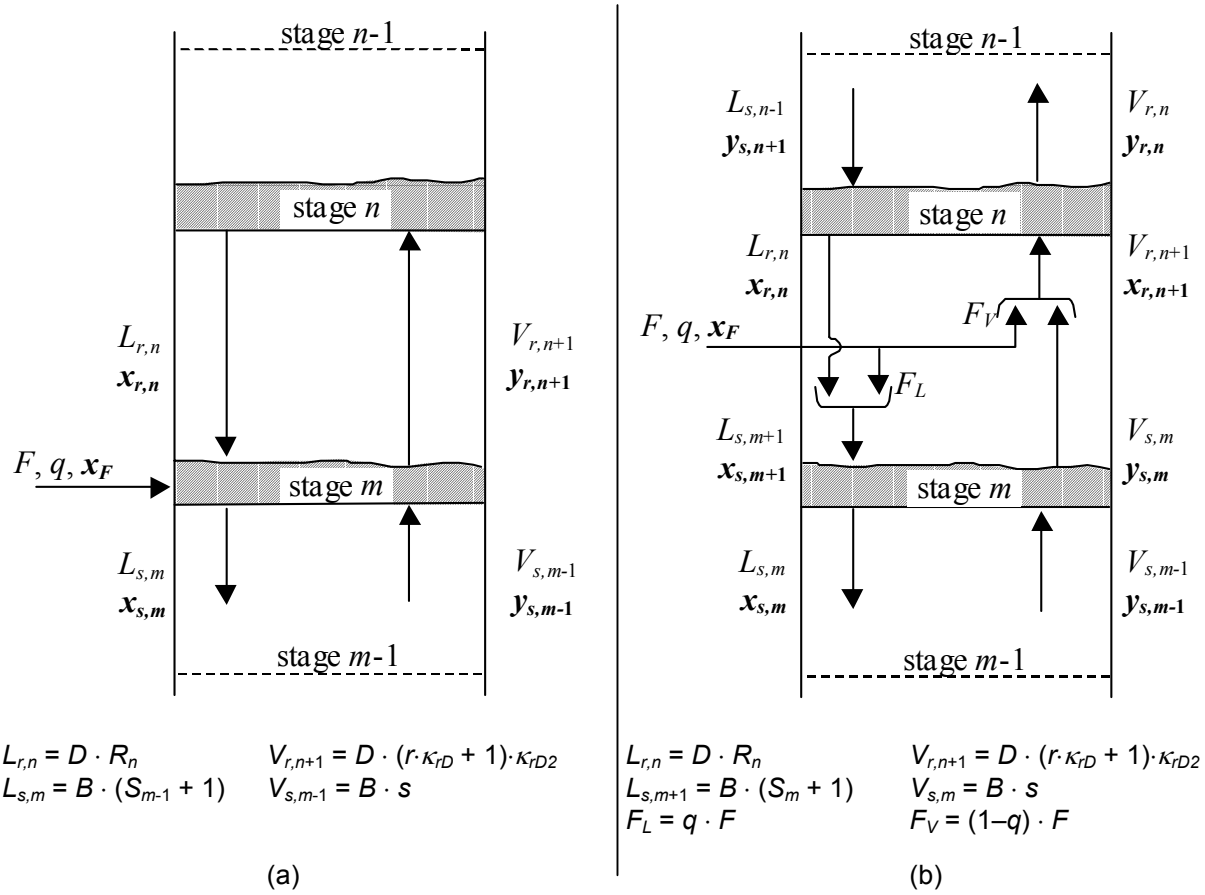

(a)

$L_{r,n} = D \cdot R_n$ $\quad V_{r,n+1} = D \cdot (r \cdot \kappa_{rD} + 1) \cdot \kappa_{rD2}$

$L_{s,m} = B \cdot (S_{m-1} + 1)$ $\quad V_{s,m-1} = B \cdot s$

(b)

$L_{r,n} = D \cdot R_n$ $\quad V_{r,n+1} = D \cdot (r \cdot \kappa_{rD} + 1) \cdot \kappa_{rD2}$

$L_{s,m+1} = B \cdot (S_m + 1)$ $\quad V_{s,m} = B \cdot s$

$F_L = q \cdot F$ $\quad F_V = (1-q) \cdot F$

Fig. 10. Feed mixing for two different feed injection points
(a) complete feed onto feed stage; (b) feed between two stages.

Furthermore, for a feasible design, a continuous composition profile must exist to connect the top and bottom product compositions. When a two-phase feed is introduced between the last stripping stage, *m*, and the last rectifying stage, *n*, the vapour fraction of the feed, F_V, mixes with the vapour leaving the feed stage, $V_{s,m}$, as shown in Fig. 10(b).

The material balances at the feed stage are:

$$V_{r,n+1} = V_{s,m} + F_V \tag{20}$$

$$L_{s,m+1} = L_{r,n} + F_L + \nu_{tot}^T \frac{d\varepsilon}{dt} \tag{21}$$

$$V_{r,n+1} \cdot y_{r,n+1,i} = V_{s,m} \cdot y_{s,m,i} + F_V \cdot y_{F_V,i} \qquad \forall\, i = 1,\ldots,C-1 \tag{22}$$

$$L_{s,m+1} \cdot x_{s,m+1,i} = L_{r,n} \cdot x_{r,n,i} + F_L \cdot x_{F_L,i} + \nu_i^T \frac{d\varepsilon}{dt} \qquad \forall\, i = 1,\ldots,C-1 \tag{23}$$

from which it follows:

$$q = \frac{B}{F} \cdot \frac{S_m + 1}{\kappa_{FB} \cdot \kappa_{sx}} - \frac{D}{F} \cdot \frac{R_n}{\kappa_{FD} \cdot \kappa_{rx}} \tag{24}$$

$$X_{s,m+1,i} = \frac{\frac{D}{F} \cdot R_n}{\frac{D}{F} \cdot R_n + q \cdot \kappa_{FD} \cdot \kappa_{rx}} \cdot X_{r,n,i} + \frac{q \cdot \kappa_{FD} \cdot \kappa_{rx}}{\frac{D}{F} \cdot R_n + q \cdot \kappa_{FD} \cdot \kappa_{rx}} \cdot X_{F_L,i}$$

$$\forall\, i = 1,\ldots,C-R-1 \tag{25}$$

and, for the vapour phase, in:

$$q = 1 + \frac{B}{F} \cdot s_1 - \frac{D}{F} \cdot (r_1 \cdot \kappa_{rD} + 1) \cdot \kappa_{rD2} \tag{26}$$

$$y_{r,n+1,i} = \frac{\frac{D}{F} \cdot (r_1 \cdot \kappa_{rD} + 1) \cdot \kappa_{rD2} - (1-q)}{\frac{D}{F} \cdot (r_1 \cdot \kappa_{rD} + 1) \cdot \kappa_{rD2}} \cdot y_{s,m,i} + \frac{1-q}{\frac{D}{F} \cdot (r_1 \cdot \kappa_{rD} + 1) \cdot \kappa_{rD2}} \cdot y_{F_V,i}$$

$$\forall\, i = 1,\ldots,C-1 \tag{27}$$

If the composition profiles of both column sections are constrained to lie in the reaction space, it is sufficient to apply either eq. (25) or (27) to establish the feasibility of the proposed separation. In non-hybrid columns, it is convenient to use the liquid phase transformed compositions (eq. 25). If different reactions take place in the column sections and, similarly, in hybrid columns, the feasibility of the proposed separation has to be checked in terms of mole fractions as well (*e.g.* eq. 27).

For a liquid feed added between two stages, the same equations as derived by Julka and Doherty [17] apply, if the liquid composition is expressed in transformed compositions:

$$X_{s,m,i} = X_{r,n+1,i} \qquad \forall\, i = 1,\ldots,C-R-1 \tag{28}$$

$$y_{s,m,i} = y_{r,n+1,i} \qquad \forall\, i = 1,\ldots,C-1 \tag{29}$$

For a vapour feed added between two stages, the criteria also apply, but the stage index has to be shifted by one stage up the column:

$$X_{s,m+1,i} = X_{r,n,i} \qquad \forall\, i = 1,\ldots,C-R-1 \tag{30}$$

$$y_{s,m+1,i} = y_{r,n,i} \qquad \forall\, i = 1,\ldots,C-1 \tag{31}$$

The new feasibility criteria (eqs. 25 and 27) reduce to the criteria derived by Julka and Doherty [17] for saturated feeds (*i.e. q* = 0 or 1). Transformed variables reduce to mole fractions if the stoichiometric coefficient of the reference components is set to zero, so that the equations are valid both in non-reactive systems and reactive systems with liquid-phase equilibrium reactions. The feasibility criteria that have to be applied for the different feed injection scenarios are summarised in Table 2.

The vapour material balance (eq. 26) for any kind of column (non-hybrid reactive, hybrid reactive and non-reactive) can relate the feed quality, *q*, to the external reflux and reboil ratios, *r* and *s*, and the ratio between the product flow rates and the feed

flow rate, *D/F* and *B/F*. The feed quality is a dependent variable. Alternatively, if the value of the feed quality is specified by the user, either the relative distillate flow rate, *D/F*, or the relative bottom product flow rate, *B/F*, is a dependent variable.

Table 2 Feasibility criteria for different feed conditions

Case	Feed location	Feed condition		Feasibility criteria
1 a	Above last stripping stage *m*	saturated or subcooled liquid	$q \geq 1$	eq. (28) eq. (29)
1 b	Above last stripping stage *m*	two-phase feed	$0 < q < 1$	eq. (25) eq. (27)
1 c	Above last stripping stage *m*	saturated or superheated vapour	$q \leq 0$	eq. (30) eq. (31)
2	Onto last stripping stage *m*	any	any	eq. (28) eq. (29)

Procedure for Feasibility Assessment and Column Design

For a given mixture, and a given system pressure, the first step is to fully specify the compositions of the distillate and bottom products and to specify the mole fraction of the *R* reference components in the feed. By choosing one design variable from *D/F, B/F* and $x_{i \neq ref}$ and closing the overall mass balance (eqs. 18 and 19), the remaining variables can calculated. Next, for a range of reflux and reboil ratios, and for a specified maximum number of stages, the composition profiles for the rectifying and stripping sections are calculated using eqs. (4) and (5). This allows the stage composition lines to be generated – linear segments are used to approximate the stage composition lines.

All pairs of segments are then tested for intersection. Initially it is assumed that the feed will be introduced between two stages. If two segments of stage composition lines intersect and the feed quality resulting from eq. (26) is negative or greater than one (a single-phase feed), then the design is feasible according to case 1a or 1c of Table 2. For line segments which do not intersect, it is necessary to check whether the mixing condition (eq. 25) is met. This condition checks whether the composition of the liquid leaving the rectifying section is collinear with a point on the stripping stage composition line and the composition of the liquid fraction of the feed. If the corresponding feed condition is a two-phase stream (*i.e.* $0 < q < 1$), then the design is feasible. If different reactions take place in the two column sections or if a hybrid columns is to be used, the feasibility of the proposed separation has to be checked in terms of mole fractions as well (*e.g.* eq. 27).

The more computationally demanding calculations entail the generation of composition profiles and flash calculations for the feed stream; other calculations involve simple geometric relationships to assess whether linear segments of stage composition lines intersect. To evaluate the designs generated, simple cost models, based on the heating and cooling demand (related to the heat of vaporisation of the product streams and to the internal flow rates) and the column capital cost (related to the number of stages and internal flow rates), can be used.

Illustration of Procedure: Non-Hybrid Reactive Distillation Columns

The automated feasibility analysis and column design procedure for systems with two degrees of freedom is illustrated using the ideal decomposition reaction presented in Table 1 and Fig. 5. Component c decomposes reversibly to products a and b in the presence of the inert component d. The physical properties of the components are reported in Appendix A.

Fig. 11 illustrates all feasible designs leading to the desired product compositions for the specified range of operating parameters and stage numbers: the composition of the liquid entering the stripping section is marked with an open circle. The designs for minimum reflux ratio, minimum reboil ratio, minimum cost and minimum number of stages are highlighted. It is interesting to note that designs corresponding to minimum reflux and reboil do not lie close to the intersection of the two pinch-point curves, but rather close to the intersection of a pinch point curve and a distillation line. Which of the many feasible design options are economically attractive can be evaluated using more or less sophisticated cost models.

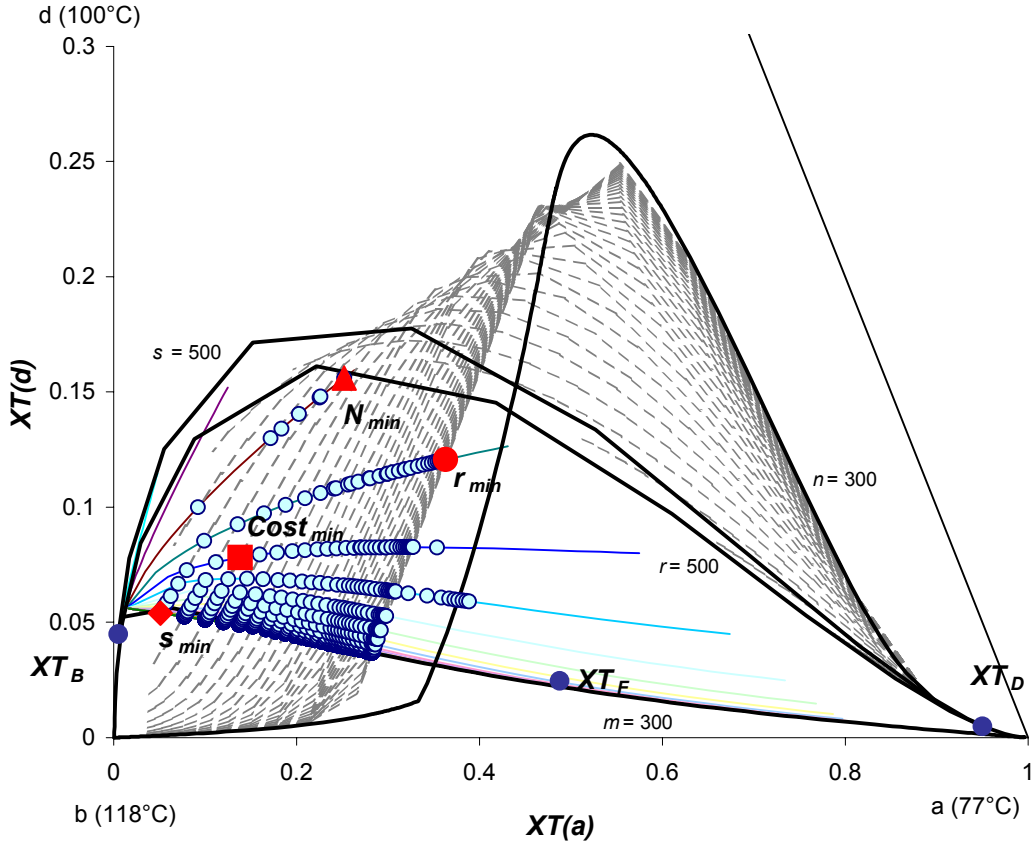

Fig. 11 Feasible designs and stage composition lines for the decomposition reaction specified in Table 1. The composition of the liquid entering the stripping section is marked. Designs of interest are highlighted.

The designs marked in Fig. 11 include all feasible designs, *i.e.* designs according to cases 1a, 1b and 1c of the feasibility criteria listed in Table 2. Feasible designs for Cases 1a and 1c are obtained from intersections of the stage composition lines. In Case 1b, there is a collinear alignment of the points on the stage composition lines with the composition of the liquid phase of the feed.

The same pair of stage composition lines may satisfy the feasibility criteria for more than one combination of reflux ratio, reboil ratio and feed quality. This means that, for a given feed composition and product specifications, a column with fixed configuration (total number of stages and feed stage location) but more than one set of operating and feed conditions can produce the desired products. Fig. 12 illustrates such a case.

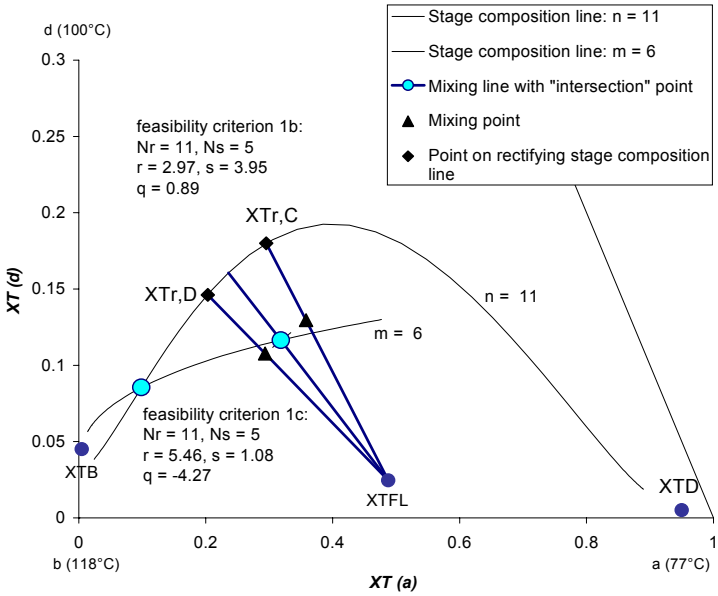

(a)

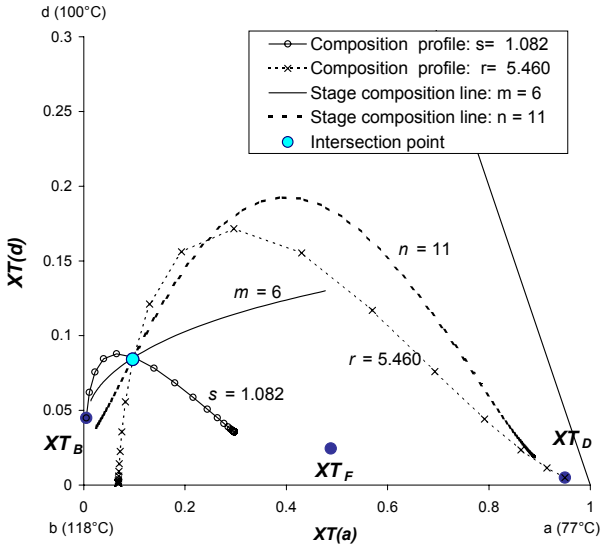

(b) Stage composition lines and composition profiles for first feasible design (criterion 1c)

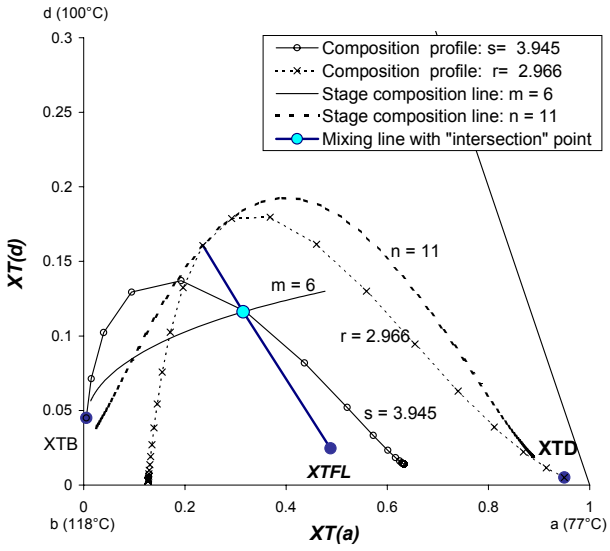

(c) Stage composition lines, composition profiles and mixing line for second feasible design (criterion 1b)

Fig. 12 Two column designs with identical configuration (N_r and N_s) but different sets of operating parameters (r, s and q) producing the same product compositions $\boldsymbol{x_D}$ and $\boldsymbol{x_B}$ from the same feed $\boldsymbol{x_F}$ (System as in Fig. 11).

One pair of rectifying and stripping stage composition lines is shown Fig. 12(a) for *n* = 11 and *m* = 6 stages. Two column designs with the same number of stages (N_r = 11

and N_s = 5) at different sets of the operating parameters *r*, *s* and *q* result from the feasibility analysis. The first set is feasible by criterion 1c, as the stage composition lines intersect and the feed quality is negative (*q* = -4.27). The second case (Fig. 12(b)) satisfies criterion 1b for a two-phase feed (*q* = 0.89). Figs. 12(b) and (c) show the stage composition lines and composition profiles for both feasible cases.

Illustration of Procedure: Hybrid Reactive Distillation Columns

The automated feasibility and design procedure for hybrid columns is illustrated for methyl tertiary butyl ether (MTBE) production. The reaction between iso-butene (IB) and methanol (MeOH) (eq. 32) takes place in the rectifying section, and pure MTBE is obtained as a bottom product. The reactive mixture contains the inert component n-butane. The calculation methods and models are described in Appendix B.

$$IB + MeOH \xleftrightarrow{\text{Cat.}} MTBE \qquad (32)$$

Fig. 13 shows the residue curve map of the reactive MTBE system in the transformed composition space. The reference component is MTBE. Two reactive azeotropes are formed: one binary light-boiling azeotrope and one quaternary saddle-azeotrope, located very close to the n-butane vertex.

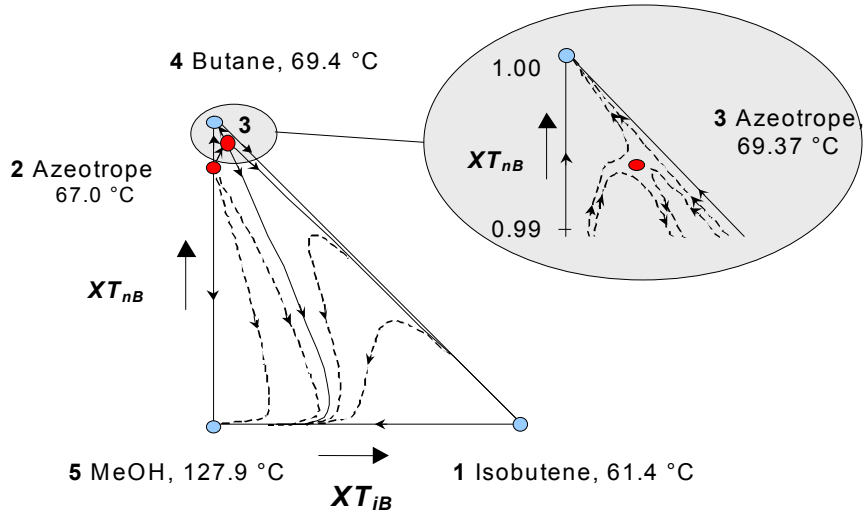

Fig. 13 Residue curve map for the reactive MTBE mixture in the transformed composition space at 8 bar. The mixture forms four distillation boundaries (solid lines).

In Fig. 14 the non-reactive azeotropes and reaction equilibrium surface is shown in mole fraction space. A distillation boundary divides the composition space into two distillation regions. Pure MTBE can only be produced from a conventional distillation column if the methanol concentration in the feed is low. The reactive residue curve map indicates that the methanol/n-butane azeotrope is a potential product composition of a reactive rectifying section. If this reactive section is combined with an inert stripping section, pure MTBE can be withdrawn as the bottom product.

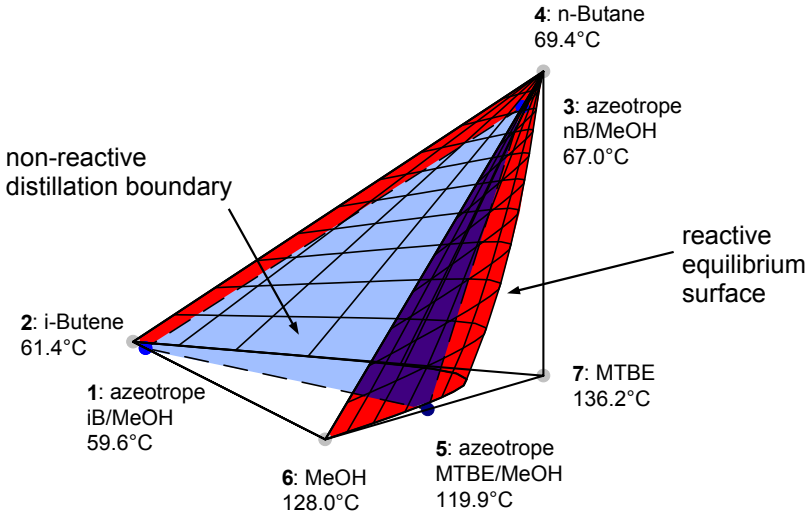

Fig. 14 Non-reactive distillation behaviour and reaction space (in mole fraction space) for the MTBE system at 8 bar. The non-reactive mixture forms three binary azeotropes, two distillation regions and one distillation boundary. The singular points are numbered in order of increasing boiling point temperature

A composition close to the quaternary reactive azeotrope is chosen as the top product, and almost pure MTBE for the bottom product. Product and feed specifications are given in Table 3. Table 4 presents the range of operating conditions used to generate reactive stage composition lines. The feed is assumed to enter the column on the last rectifying stage (case 2 in Table 2).

Table 3 Products and feed compositions for MTBE example

Comp.	Stoichiometry	Non-reactive boiling temp. at 8 bar	Distillate		Bottoms		Feed	
	ν	T_B	X_D	x_D	X_B	x_B	X_F	x_F
	[-]	[°C]	transf.	mole fr.	transf.	mole fr.	transf.	mole fr.
i-Butene	-1	61.4	0.12(#)	0.1124	0.494(#)	0.0001	0.2698	0.2698
MeOH	-1	128.0	0.1(#)	0.0015	0.504(#)	0.0195	0.2077	0.2077
MTBE	1	136.4	0.0(#)	0.0086	0.0(#)	0.9781	0.0	0.0(#)
n-Butane	0	69.4	0.87(#)	0.8775	0.012(#)	0.0023	0.5225	0.5225(#)

(#) *specified values*

Table 4 Specifications for generating stage composition lines

Distillate flowrate	Bottoms flowrate	Feed flowrate	Feed quality	Reflux ratio range	Reboil ratio range	Rectifying stages range	Stripping stages range
D/F	*B/F*	*F*	*q*	*r*	*s*	*n*	*m*
[-]	[-]	[kmol/h]	[-]	[-]	[-]	[-]	[-]
0.5949	0.2022	100	from Eq. 24	0.1 – 15	0.1 – 15	1 – 30	1 - 30

For hybrid reactive distillation columns, the procedure for generating feasible column designs is similar to that used for non-hybrid columns. The stage composition lines for the rectifying and stripping sections are calculated in transformed composition

space. Intersection between a rectifying and a stripping stage composition line indicates a potentially feasible design. Because the composition space in a non-reactive stripping section has one additional dimension, compared with the composition space of the reactive rectifying section, an additional feasibility criterion has to be satisfied; in this example it is the mass balance for the reference component at the intersection point (eq. 33, cf. Fig. 9).

$$L_{s,m+1} \cdot x_{s,m+1,ref} = V_{s,m} \cdot y_{s,m,ref} + B \cdot x_{B,ref} \qquad (33)$$

Fig. 15 shows ten feasible designs for the hybrid reactive distillation column, and two designs corresponding to a saturated liquid feed that are obtained by interpolation. The parameters for these designs are given in Tables 5 and 6. These designs are easily evaluated, using appropriate cost models.

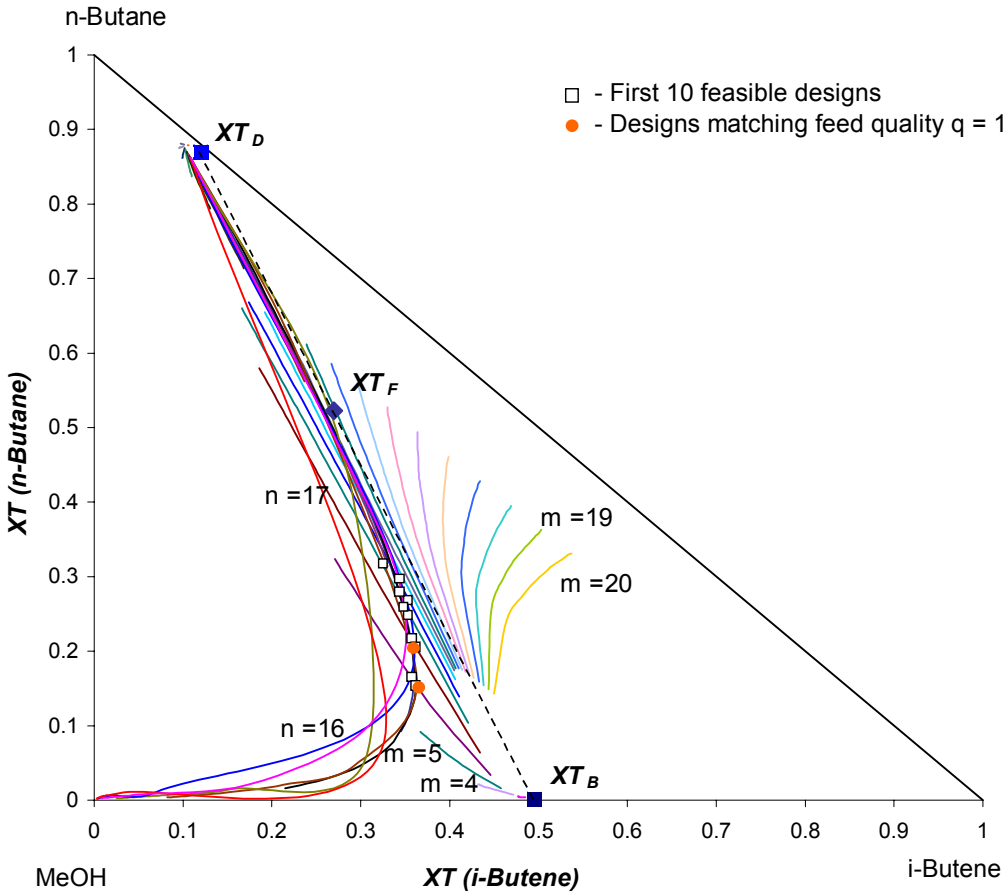

Fig. 15 Stage composition lines and feasible designs for MTBE synthesis

Because the distillate composition is very close to the quaternary reactive azeotrope, the feasible designs are grouped close to a distillation boundary, as can be seen in Fig. 15. For the feasibility study, small steps for reflux and reboil ratios are needed to generate the stage composition lines near to the distillation boundary accurately.

Table 5 Feasible designs for MTBE production

No	Reflux Ratio [-]	Reboil Ratio [-]	q [-]	N_r [-]	N_s [-]	$N_r + N_s$ [-]	Condenser Duty [kW]	Reboiler Duty [kW]	Diameter [m]	Height [m]
1	2.41	2.64	-0.50	16	5	21	1097	383	1.29	13.2
2	2.59	2.32	-0.67	15	7	22	1155	336	1.32	13.7
3	2.64	2.47	-0.67	15	6	21	1171	357	1.33	13.2
4	2.56	2.32	-0.65	15	8	23	1144	335	1.31	14.1
5	2.72	3.40	-0.53	15	5	20	1197	492	1.34	12.7
6	1.97	4.01	0.05	16	6	22	953	580	1.20	13.7
7	3.81	2.72	-1.31	13	5	18	1545	394	1.53	11.8
8	3.42	2.96	-1.03	13	6	19	1420	428	1.46	12.3
9	2.84	3.59	-0.56	14	6	20	1234	519	1.37	12.7
10	4.39	2.29	-1.74	12	7	19	1731	332	1.62	12.3

Table 6 Feasible designs for MTBE synthesis matching feed condition q = 1

No	Reflux Ratio [-]	Reboil Ratio [-]	q [-]	N_r [-]	N_s [-]	$N_r + N_s$ [-]	Condenser Duty [kW]	Reboiler Duty [kW]	Diameter [m]	Height [m]
1	1.94	8.66	1	16.6	5	21.6	946	1248	1.45	13.5
2	1.76	8.11	1	16.4	6	22.4	885	1168	1.38	13.8

Design 1 from Table 6 is used to initialise a rigorous simulation using HYSYS 2.4 [19], using 17 stages in the rectifying section and 5 stages in the stripping section. The results of the conceptual design method were used to specify the reactive column; the product compositions predicted by simulation are compared to those specified in the conceptual design method in Table 7. The simulation shows good agreement with the conceptual design method.

Table 7 Product compositions obtained by simulation, based on the results from the conceptual design procedure

	Simulation results			Conceptual design specifications		
Component	x_F	x_D	x_B	x_F	x_D	x_B
i-Butene	0.2698	0.1061	1.45E-05	0.2698	0.1124	0.0001
MeOH	0.2077	2.54E-04	9.49E-05	0.2077	0.0015	0.0195
MTBE	0	2.73E-03	0.9998	0.0	0.0086	0.9781
n-Butane	0.5225	0.8909	6.97E-05	0.5225	0.8775	0.0023

CONCLUSIONS

A new graphical design methodology has been developed to assess feasibility and design columns for proposed reactive distillation processes. The methodology is restricted to systems with two degrees of freedom and single-feed two-product columns; it is assumed that equilibrium reactions take place in the liquid phase only. Further assumptions of constant molar overflow in the vapour phase and no pressure drop in the column are not fundamental to the approach.

Reactive stage composition lines, defined by analogy with non-reactive stage composition lines, are defined to describe the liquid composition on a given stage, for any reflux or reboil ratio. Established criteria to assess feasibility of a proposed pair of products are reformulated in terms of reactive stage composition lines, and extended to account for the case where a two-phase feed is introduced between two stages. The advantage of using stage compositions lines, rather than composition profiles, for design, is that they are continuous in nature. Intersection of stage composition lines is therefore more meaningful for assessing designs or initialising rigorous simulations.

Feasibility criteria in terms of transformed compositions are used for fully reactive columns. For hybrid columns, in which reaction takes place in one or the other of the two column sections, and for columns in which different reactions take place in the two column sections, an additional feasibility relationship, expressed in terms of mole fractions, must also be satisfied.

The new methodology is easily automated and typically generates multiple designs. It overcomes some of the limitations and inaccuracies of previous approaches for assessing feasibility and designing simple reactive distillation columns with two degrees of freedom and equilibrium reactions. The approach does not require iteration to obtain converged column profiles, and is efficient in the way that information obtained from composition profiles is used. Both fully reactive and hybrid columns, as well as non-reactive columns, can be accommodated. The approach allows the feed to be introduced to a single stage or between two stages. The multiple designs that are obtained can be evaluated using appropriate cost models.

APPENDIX A Physical property data for the ideal system a, b, c, d

The reaction a + b $\longleftrightarrow$ c takes place in the presence of inert component d. The chemical equilibrium constant, K_{Eq}, is 1. Component c is the reference component. All activity and fugacity coefficients are unity. The Antoine equation is used to calculate vapour pressure:

$$\ln\left(P_i^{sat}\right) = a_i - \frac{b_i}{T + c_i} \qquad P \text{ in [kPa] and } T \text{ in [K].} \qquad \text{(A1)}$$

Parameters for the Antoine equation are taken from Barbosa and Doherty [3]:

Table A1 Antoine parameters and normal boiling points for components in the ideal decomposition reaction.

Component	a_i [-]	b_i [K]	c_i [K]	T_B [°C]
a	9.73229	2866.606	– 55.279	77
c	12.05885	3667.705	– 46.976	78
d	11.96469	3984.923	– 39.734	100
b	10.39090	3530.584	– 50.851	118

APPENDIX B Physical Property Data for MTBE System

Components: iso-butene (IB; i-C_4H_8), methanol (MeOH; CH_3OH), methyl tertiary butyl ether (MTBE; $(CH_3)_3COCH_3$), and the inert component n-butane (n-B; n-C_4H_{10}).

$$\mathrm{IB} + \mathrm{MeOH} \xleftrightarrow{\text{Cat.}} \mathrm{MTBE}$$

The Wilson model is used to calculate activity coefficients in the liquid phase. HYSYS [19] is used to calculate all properties of the reactive mixture.

The reaction equilibrium expression is taken from Thiel *et al.* [20]:

$$\begin{aligned}\ln\left(K_{Eq}\right) = \ln 284 &- 1.49277\cdot 10^{3}\cdot\left(\frac{1}{T}-\frac{1}{298.15}\right) - 7.74002\cdot 10^{1}\cdot\ln\left(\frac{T}{298.15}\right)\\ &+ 5.07563\cdot 10^{-1}\cdot\left(T-298.15\right) - 9.12739\cdot 10^{-4}\cdot\left(T^{2}-298.15^{2}\right)\\ &+ 1.10649\cdot 10^{-6}\cdot\left(T^{3}-298.15^{3}\right) - 6.27996\cdot 10^{-10}\cdot\left(T^{4}-298.15^{4}\right)\end{aligned}$$

where T is temperature in K.

NOMENCLATURE

a_i	activity of component i
B	molar flow rate of bottom product
C	number of components
D	molar flow rate of distillate
F	molar flow rate of feed
k_f	reaction rate constant
K_{Eq}	thermodynamic equilibrium constant
L	molar flow rate of liquid
N_r	number of rectifying stages
N_s	number of stripping stages
q	feed quality (heat required to produce saturated liquid feed/molar latent heat of feed)
r	reflux ratio
R	number of reactions
R	transformed reflux ratio
s	reboil ratio
S	transformed reboil ratio
t	residence time
T	temperature (in K)
T_B	boiling temperature (°C)
V	molar flow rate of vapour
x_i	mole fraction of component i
x_{ref}	column vector of R reference component mole fractions
X_i	transformed composition of component i
XT_i	transformed composition of component i

Greek letters

ε	molar extent of reaction

κ dimensionless parameters defined in eqs. (6) to (11)
ν_i column vector of R stoichiometric coefficients for component i
ν_{tot} column vector of R sums of stoichiometric coefficients
ν_{ref} square matrix of R stoichiometric coefficients for the R reference components in the R reactions
π number of phases

Subscripts and superscripts
B bottom product
D distillate
F feed
i component i
m stage m (stripping section)
n stage n (rectifying section)
ref reference component
T transformed
tot total (over all components)

REFERENCES

1. B. Bessling and G. Schembecker, K. H. Simmrock (1997), *Ind. Eng. Chem. Res.* **36**, 3032-3042.

2. S. M. Wales (1985), *Phase Equilibrium Chemical Engineering*, Butterworth, Boston, MA.

3. D. Barbosa and M. F. Doherty (1988), *Chem. Eng. Sci.* **43**, 1523-1537.

4. S. Ung and M. F. Doherty (1995), *Chem. Eng. Sci.* **50**, 23-48.

5. J. Espinosa, P. A. Aguirre and G. A. Perez (1995), *Ind. Eng. Chem. Res.* **34**, 853-861.

6. D. Y. C. Thong, F. J. L. Castillo and G. P. Towler (2000), *Chem. Eng. Sci.* **55**, 625-640.

7. O. M. Wahnschafft, J. W. Koehler, E. Blass and A. W. Westerberg (1992), *Ind. Eng. Chem. Res.* **32**, 1121-1141.

8. F. J. L. Castillo (1997), *Synthesis of Homogeneous Azeotropic Distillation Sequences*, Ph.D. Thesis, UMIST, UK.

9. S. Ung and M. F. Doherty (1995), *AIChE J.* **41**, 2383-2392.

10. D. Barbosa and M. F. Doherty (1988), *Chem. Eng. Sci.* **43**, 2377-2389.

11. J. Espinosa, P. A. Aguirre and G. A. Perez (1995), *Chem. Eng. Sci.* **50**, 469-484.

12. T. E. Güttinger and M. Morari (1999), *Ind. Eng. Chem. Res.* **38**, 1649-1665.

13. G. Buzad and M. F. Doherty (1995), *Comp. Chem. Eng.*, **19(4)**, 395-408.

14. M. J. Okasinski and M. F. Doherty (1998), *Ind. Eng. Chem. Res.* **37**, 2821-2834.

15. S. M. Mahajani (1999), *Chem. Eng. Sci.* **54**, 1425-1430.

16. S. Melles, J. Grievink and S. M. Schrans (2000), *Chem. Eng. Sci.* **55**, 2089-2097.

17. V. Julka and M. F. Doherty (1990), *Chem. Eng. Sci.* **45**, 1801-1822.

18. H. Z. Kister (1992), *Distillation Design*. McGraw-Hill.

19. HYSYS 2.4.1 (1995 – 2001), AEA Technology Engineering Software, Hyprotech Ltd, Calgary, Canada.

20. C. Thiel, K. Sundmacher and U. Hoffmann (1997), *Chem. Eng. Sci.* **52**, 993-1005.